



Magnetotelluric transect across the Niigata-Kobe Tectonic Zone, central Japan: A clear correlation between strain accumulation and resistivity structure

R. Yoshimura,¹ N. Oshiman,¹ M. Uyeshima,² H. Toh,^{3,4} T. Uto,¹ H. Kanezaki,³ Y. Mochido,⁵ K. Aizawa,² Y. Ogawa,⁶ T. Nishitani,⁷ S. Sakanaka,⁷ M. Mishina,⁸ H. Satoh,^{9,10} T. Goto,^{11,12} T. Kasaya,¹¹ S. Yamaguchi,¹³ H. Murakami,¹⁴ T. Mogi,¹⁵ Y. Yamaya,¹⁵ M. Harada,¹⁶ I. Shiozaki,⁵ Y. Honkura,¹⁷ S. Koyama,² S. Nakao,¹ Y. Wada,¹ and Y. Fujita¹

Received 16 July 2009; revised 3 September 2009; accepted 15 September 2009; published 23 October 2009.

[1] We obtained an electrical transect image of the Niigata-Kobe Tectonic Zone (NKTZ). Several major active faults are located in this zone of concentrated deformation. The main features of the final two-dimensional model are a thick resistive block in the upper crust, with a thinned-out portion beneath the Atotsugawa Fault, and a strong conductor in the lower crust that intrudes upward into the upper resistor. The upper crustal resistive zone corresponds well to the spatiality of the NKTZ, and relatively conductive zones sandwiching this resistor may contribute to observed changes in displacement rates. The overlapping locations of the conductor and the low-velocity body in the lower crust indicate that the conductor represents a zone that was weakened by fluids. Given that microearthquakes are localized in the regions between the resistive and conductive zones, we suggest that the distribution of earthquakes is influenced by intrusions of fluid derived from the conductor. **Citation:** Yoshimura, R., et al. (2009), Magnetotelluric transect across the Niigata-Kobe Tectonic Zone, central Japan: A clear correlation between strain accumulation and resistivity structure, *Geophys. Res. Lett.*, 36, L20311, doi:10.1029/2009GL040016.

1. Introduction

[2] The Japanese dense geodetic network, based on Global Positioning System (GPS) observations, has recently revealed a deformation belt with high strain rates, known as the Niigata-Kobe Tectonic Zone (NKTZ) [Sagiya *et al.*, 2000]. The NKTZ, about 500 km long and 50–100 km wide, is located in the northern parts of the Chubu and Kinki districts (see the inset map in Figure 1). The area in and around this zone is characterized by historical earthquakes and a concentration of major active faults. Several

models have been proposed to explain the relationship between these seismic events and the zone of concentrated deformation, and to figure out the origin of the NKTZ [e.g., Iio *et al.*, 2002; Hyodo and Hirahara, 2003]. To test the validity of these models, it is important to investigate the heterogeneous structure beneath the NKTZ. A multidisciplinary research project was initiated in 2004 to investigate the area around the NKTZ, especially the Atotsugawa fault system, based on dense GPS and seismological observations, and electromagnetic surveys. As shown in Figure 1, the Atotsugawa fault system consists of three right-lateral strike-slip faults (the Atotsugawa (AF), Mozumi–Sukenobe (MSF), and Ushikubi faults (UF)) that strike approximately N60°E. In addition, the aligned seismicity, along the Takayama–Oppara Fault Zone (TOFZ), is clearly recognized about 30 km southwest of the AF [Ito *et al.*, 2007].

[3] In a previous electromagnetic study, Goto *et al.* [2005] undertook wideband magnetotelluric (WMT) measurements around the AF. The authors established two profiles of WMT soundings with the aim of quantifying the nature of seismic heterogeneity along the AF. Spatially heterogeneous seismicity is clearly recognized along the AF, with low seismic activity along the central segment compared with the outer segments [e.g., Mikumo *et al.*, 1988; Ito *et al.*, 2007]. Goto *et al.* [2005] explained these heterogeneities in terms of the presence or absence of structural contrast in the upper crust. Although their image around the AF is of value, the spatial resolution is not high enough to enable comparisons with GPS results and seismogenic models. Thus, to discuss the role of active faults in the NKTZ, it is necessary to obtain a higher-resolution electrical image of the lower half of the crust, along a longer transect. Here, we report on new WMT data collected across the AF system in 2004 as a part of a multidisciplinary

¹DPRI, Kyoto University, Uji, Japan.

²ERI, University of Tokyo, Tokyo, Japan.

³Department of Earth Sciences, University of Toyama, Toyama, Japan.

⁴Now at Graduate School of Science, Kyoto University, Kyoto, Japan.

⁵Department of Civil Engineering, Tottori University, Tottori, Japan.

⁶VFRC, Tokyo Institute of Technology, Tokyo, Japan.

⁷Department of Earth Science and Technology, Akita University, Akita, Japan.

⁸RCPEVE, Tohoku University, Sendai, Japan.

⁹AIST, Tsukuba, Japan.

¹⁰Now at Nippon Engineering Consultants Co., LTD, Tokyo, Japan.

¹¹JAMSTEC, Yokosuka, Japan.

¹²Now at Department of Civil and Earth Resources Engineering, Kyoto University, Kyoto, Japan.

¹³Department of Earth and Planetary Sciences, Kobe University, Kobe, Japan.

¹⁴Department of Applied Science, Kochi University, Kochi, Japan.

¹⁵ISV, Hokkaido University, Sapporo, Japan.

¹⁶EPRC, Tokai University, Shizuoka, Japan.

¹⁷Department of Earth and Planetary Sciences, Tokyo Institute of Technology, Tokyo, Japan.

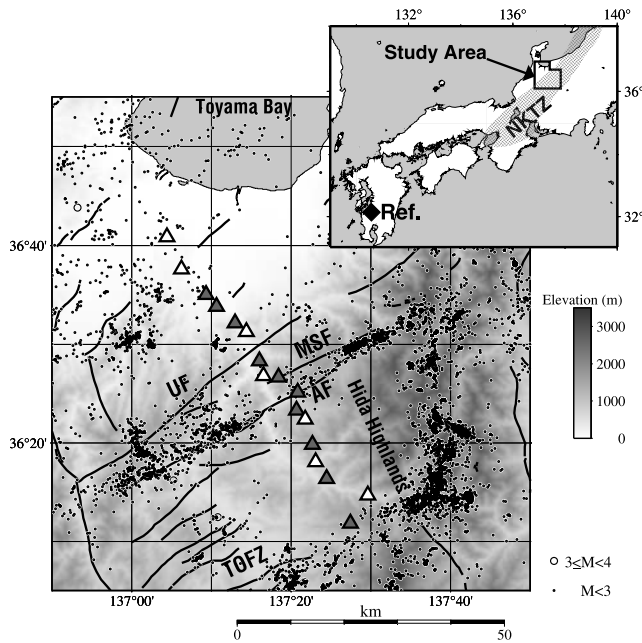


Figure 1. Topographic map of the study area. The epicenters of microearthquakes determined by the Kamitakara Observatory (DPRI, Kyoto University Japan) are plotted as circles scaled to earthquake magnitude (for the period January 2000 to May 2004). Several active faults are shown as thick lines. Gray and white triangles represent five/four-component magnetotelluric (MT) sites and electric-field-only MT sites, respectively. The NKTZ [Sagiya *et al.*, 2000] is shown as the shaded area in the inset map. The black diamond indicates the remote reference site employed for MT data processing.

research project. The data were collected along a long profile with a dense distribution of WMT sites, along the eastern profile of previous surveys (Profile B–B' by Goto *et al.* [2005]). The present profile passes through the relatively low-seismicity segment and the deepest area of the seismicity cutoff along the AF. In this paper, we concentrate on the wider area, and we present a deep-level two-dimensional electrical interpretation and discuss the relationship between crustal structure and the zone of concentrated deformation.

2. Data Acquisition and Analysis

2.1. Magnetotelluric Measurements

[4] In October 2004, we carried out WMT measurements at 17 sites across the central part of the NKTZ, where a number of active faults are located (UF, MSF, AF, and TOFZ). The locations of the WMT sites are shown in Figure 1, along with recent seismic activity. In this campaign, we used five-component (three magnetic and two telluric channels) and two-component (two telluric channels) WMT instruments (MTU5 and MTU2E systems, respectively; Phoenix Geophysics Ltd.) at 10 and 7 sites, respectively. Electromagnetic field data were recorded in the frequency range from 320 Hz to 5×10^{-4} Hz and synchronized via signals from GPS satellites. An important improvement in the present version of instruments compared with those used in earlier surveys [Goto *et al.*, 2005] is the use of 24-bit

analog-to-digital converters, which provide a wide dynamic range and enabled us to obtain accurate low-frequency MT signals. We also measured magnetic field data at a site located approximately 800 km southwest of the study area (see the inset map in Figure 1) in order to apply the remote reference technique [Gamble *et al.*, 1979] for reducing the effects of artificial local noise.

2.2. Data Processing and Sorting for Modeling

[5] We calculated MT responses using only nighttime data (23:00–06:00 Local Time), as an analysis of longitudinal data revealed that spiky noises due to leakage currents from DC electric railways dropped during the nighttime. At telluric-only sites, magnetic field data were taken from nearby sites with high-quality data.

[6] After calculating the MT responses, we investigated the two-dimensionality of the data and determined the strike direction for two-dimensional inversion by phase-tensor analysis [Caldwell *et al.*, 2004]. Figures 2a–2c show the cumulative principal directions of the phase-tensor, which are aligned parallel or perpendicular to the geoelectrical strike in the two-dimensional case. The data show concentrations at $N65^\circ E$, especially at the frequency range lower than 1 Hz (Figure 2b). This direction is approximately parallel to the strike of active faults in the area ($N60^\circ E$) and the trend of the NKTZ. Because we sought to image the deep structure over a wide area, we adopted a geoelectrical strike of $N65^\circ E$, consistent with the strike estimated in a previous study [Goto *et al.*, 2005]. However, the skew angles of the phase-tensor (Figures 2d–2f), which measure the asymmetry of the phase response, indicate that some data were affected by three-dimensional structure. In particular, the use of TE mode data for two-dimensional inversions is not appropriate in the three-dimensional case, for which TM mode data are more robust [e.g., Wannamaker, 1999; Siripunvaraporn *et al.*, 2005]. Consequently, we placed a limit on the use of TE mode data for two-dimensional inversion. In the inversion procedure, we excluded the TE mode phase responses with large phase-tensor skew angles (exceeding 6°), and the apparent resistivities.

3. Two-Dimensional Modeling

[7] To implement the two-dimensional inversion, we rotated the impedance tensors $65^\circ E$ to the estimated geoelectric strike direction and classified their off-diagonal terms into TM and TE modes (i.e., electrical field oriented perpendicular or parallel to the strike, respectively). We inverted the apparent resistivity data and phase of TM mode, some phases of TE mode data and the vertical magnetic field using the code developed by Ogawa and Uchida [1996]. The data adopted for the inversion procedure are indicated by dots in the upper panels of Figure 3b. In the inversion, the error floor values for the apparent resistivity and tipper were set at 5%, and equivalent values were set for the phase. The modeling took into account the different locations of the telluric and magnetic fields at telluric-only sites. Figure 3a shows the best-fit resistivity model within $10^{0.3}$ of the standard deviation of the estimated resistivity block. The root-mean-square (RMS) value of the inversion converged to 1.57, and we obtained a good fit between observed and calculated responses (Figure 3b). We

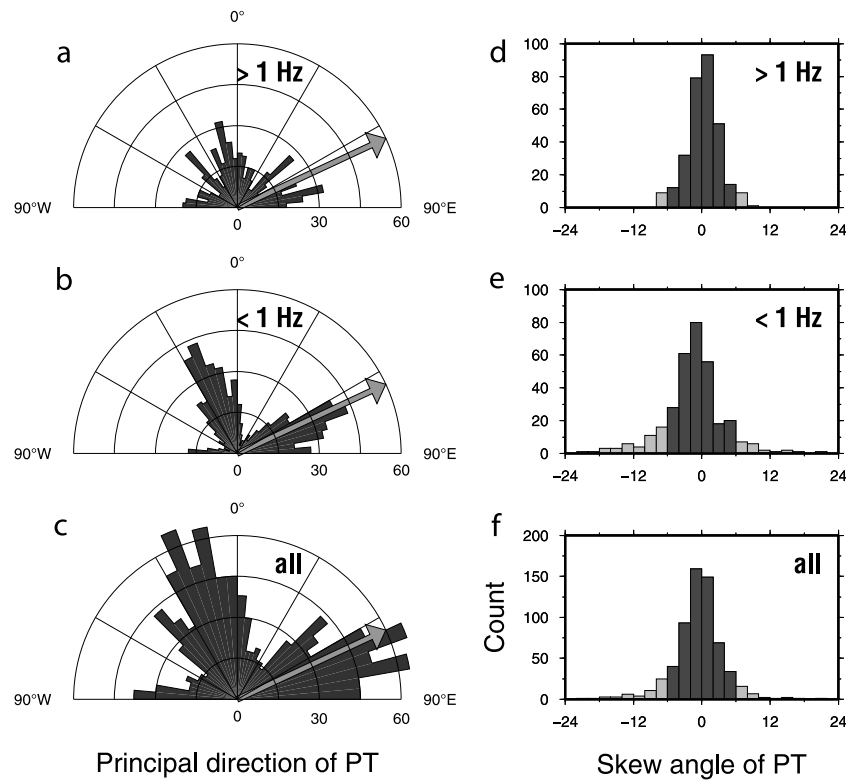


Figure 2. Rose diagrams and histograms of directional parameters for the respective frequency bands. (a–c) Cumulative principal directions (α) of the phase-tensor (PT) analysis [Caldwell *et al.*, 2004] are shown with a 90° ambiguity. The estimated strike for modeling, $N65^\circ E$, is indicated by arrows. (d–f) Cumulative skew angles (β) of the PT, which represent the asymmetry of the phase response produced by the three-dimensional structure. The data have sizable β values ($|\beta| > 6^\circ$), shown as gray bars, which placed a limit on the use of the inversion procedure.

also confirmed that a similar model was obtained using the inversion code of *Siripunvaraporn and Egbert* [2000].

4. Discussion and Conclusions

[8] First, we compare our final model with the image obtained in a previous study [Goto *et al.*, 2005]. Although the two images share certain similarities, in that a resistive block (R1) of wide extent is estimated at a depth of about 5 km, its northward extension is clearly detected in the present study. Another significant aspect of deeper structure resolved in our model is an undulation in the depth range of resistivity contrast, from 5 to 15 km. The main reason for these improvements is that the wider and denser WMT of the present study enabled us to resolve the fine electrical structure.

[9] Next, we interpret the major features of the obtained model with reference to other geophysical data. In the northern part of the WMT profile, a high conductive layer (C1) is detected at shallow depths. This region corresponds to the coastal plain around Toyama Bay, confirming the existence of a thick sedimentary layer, estimated to be approximately 3 km thick based on seismic experiment data [e.g., Ueno *et al.*, 2005]. The thick conductive layer has also similarity to the seismic tomography result [Kato *et al.*, 2006], and is therefore attributed to pore fluids within the sediment.

[10] A highly resistive block (R1) is widespread in the upper and middle crust (from the surface to a depth of 15 km) beneath the mountainous area (Hida Highlands). The northern and southern margins of the block appear to coincide with the locations of UF and TOFZ. The resistive

layer shows a gradual thinning to approximately 5 km thickness at the AF and MSF, as though it is bending upward at these zones. A zone of low resistivity (C2) is clearly imaged beneath this thinned-out portion, extending from the lower crust to the bottom of the upper-crustal resistor (R1). The existence of vertical low-resistivity zones (BC1 and BC2) at the margins of the resistor (R1), a convex geometry of its lower bound and the presence of the deep-seated conductor (C2) are made certain of being sufficiently sensitive by several forward tests.

[11] Investigation of a surface geological map [Geological Survey of Japan, 2007] reveals that the Hida granitic and metamorphic (mainly gneiss) rocks are widespread above the resistive zone (R1). Given that laboratory measurements have demonstrated that granitoids and gneiss show high resistivity ($> 10^3 \Omega m$) under dry conditions and mid-crustal temperatures [e.g., Kariya and Shankland, 1983; Fuji-ta *et al.*, 2007], the resistor (R1) probably corresponds to the distribution of these rocks. The estimated resistivity range of R1 does not require strongly inter-connected fluids or high porosity, and such a resistive zone may behave as a rigid elastic block. Seismic tomography around the study area [Kato *et al.*, 2006] also detected a high-velocity zone corresponding to the resistive block (R1), thereby supporting the interpretation of a rigid zone depleted in fluids. In contrast, the relatively conductive zones (BC1 and BC2) at the margins of the resistor (R1) necessitate enhanced fluid-bearing porosities, given their resistivities of less than $100 \Omega m$; such conductive zones have the potential to accommodate intense deformation.

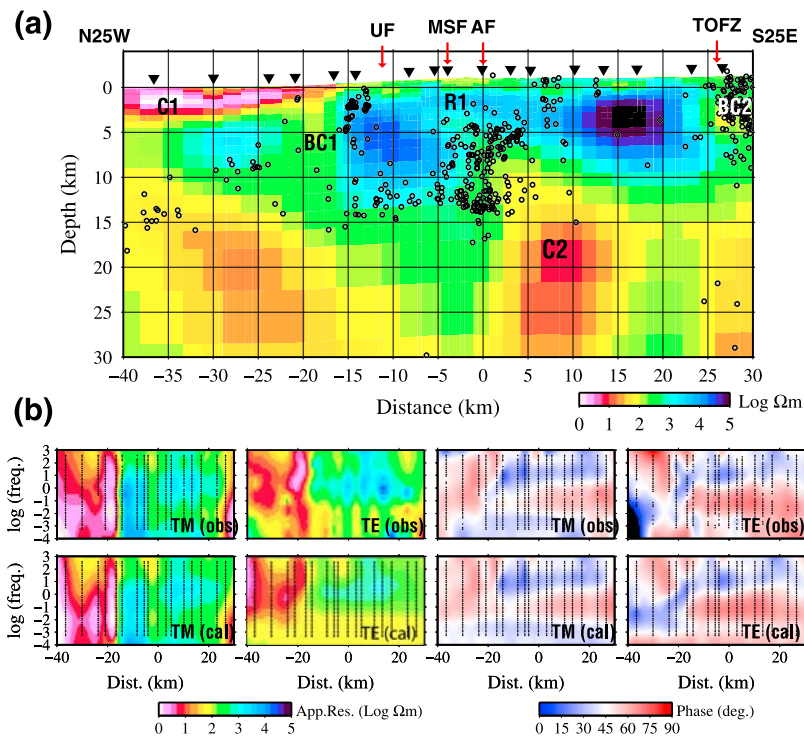


Figure 3. (a) Two-dimensional resistivity model obtained along the 70 km MT profile across the NKTZ. Inverted triangles indicate the locations of the MT sites. Seismic activity located close to the study area [Ito *et al.*, 2007], within ± 10 km of the section line, is shown by open circles. Red arrows with abbreviations indicate the locations of the surface traces of active faults. Features labeled C1, C2, R1, BC1, and BC2 are discussed in the text. (b) MT pseudo-sections of the (top) observed responses and (bottom) calculated responses from the final model. Dots represent the data used in the inversion procedure.

[12] Based on data from a dense across-fault GPS array, Hirahara *et al.* [2003] reported a gradual change in displacement rate between the UF and TOFZ, whose spatial distribution corresponds well with that of the resistive zone (R1). The authors explained the obtained features of the rate field in terms of a simple collision model involving elastic upper-crustal blocks with a thickness of 15 km. However, they noted that the northern side of UF (coincident with BC1) requires lower elasticity or inelastic properties in order to model the observed anomalous rate vectors. The obtained laterally heterogeneous MT image in the upper crust endorses the requirement of elasticity variations or inelastic zones. In addition, we note that the thinned-out portion of the resistive block retains the potential to contribute to small-scale deformation under the effect of regional tectonic loading.

[13] In terms of electrical structure in the lower crust, we detected several conductors to which the heterogeneous features in the upper crust extend. In particular, a conductor (C2) jutting into the upper crustal resistive body (R1) is estimated beneath the AF. Wide-area seismic tomography [Nakajima and Hasegawa, 2007] has revealed a distinct low-velocity region corresponding to C2. This region is marked by a moderate heat flow of 75 mW/m^2 [Uyeda and Horai, 1964], while there are Quaternary volcanoes (Tateyama and Hakusan) at both extensions of the AF. Furthermore, previous seismic experiments recorded distinct reflectors below the AF [Ueno *et al.*, 2005]; in particular, one of the reflectors was estimated to occur at a depth of 11 km, corresponding to the top of the conductor

(C2). These correlations suggest that the lower crustal conductor (C2) represents a fluid-filled zone.

[14] Assuming the presence of a saline fluid (approximately $0.04 \text{ } \Omega\text{m}$, equivalent to 3.6 wt% KCl [Nesbitt, 1993]), it is possible to estimate the range in porosity around the conductor (C2) using the modified Archie's law [Glover *et al.*, 2000] as a mixing model. The calculations reveal that a porosity range of 0.5–6.9% under connectivity of $m = 1\text{--}2$ for the conducting (usually fluid) phase is required to explain the observed resistivity value in the lowest-resistivity region of C2. Although the estimation of porosity depends on the properties of the pore fluids, the lateral heterogeneity in electrical properties in the lower crust raises the possibility of spatial variations in porosity (up to a few percent) or pore connectivity. Thus, we speculate that the conductive zone (C2) with a low-velocity anomaly represents a rheologically weak zone due to relatively high water content in the lower crust.

[15] Iio *et al.* [2002] proposed that the lower-crustal weak zone plays a key role in terms of determining the dominant deformation mechanism beneath the NKTZ. In other MT surveys, Ogawa and Honkura [2004] also revealed conductors in the lower crust that correspond to zones of strongly negative dilatation around the Itoigawa–Shizuoka Tectonic Line. The similar nature of these various images beneath high-strain regions indicates that the presence of lower-crustal conductors plays a role in forming zones of high strain. However, in constructing a kinetic model, it is necessary to take into account the contributions of not only lower-crustal weak zones, but also heterogeneity in the upper crust, as noted above.

[16] In Figure 3a, earthquake hypocenters determined by dense seismic observations [Ito *et al.*, 2007] are superimposed onto the obtained resistivity image. It is clear that these earthquakes are located near the bottom of the resistor (R1) and therefore near the top of the lower crustal conductor (C2), as well as near the northern and southern edges of the resistor. Previous MT surveys conducted in areas characterized by intraplate earthquakes have revealed seismogenic regions close to structural discontinuities, and the location of conductors near these discontinuities highlights the relevance of the presence of fluids to the distribution of seismic activity [e.g., Ogawa *et al.*, 2001; Güner and Bayrak, 2007; Yoshimura *et al.*, 2008]. In the present study, we conclude that the conductor (C2) represents a fluid-filled zone. Hence, the earthquake occurrences may be involved by fluid intrusions from the deep-seated conductor into the brittle zone. The fact that the heterogeneous electrical features show a close spatial relationship with the distribution of the displacement rate and with seismicity suggests that the resistivity image can be used as an index from which to evaluate the deformation characteristics of the crust.

[17] **Acknowledgments.** We would like to thank the landowners who kindly provided access to their properties for geophysical measurements. Seismic data were provided by K. Ito and H. Wada of DPRI, Kyoto University. We are grateful to Y. Kuwaba, Y. Tanaka, N. Ujihara, T. Nagano, M. Hata, T. Motobayashi, Y. Matsuura, S. Moritani, and H. Kasami for their assistance in the field. K. Yokoi of Nittetsu Mining Consultants Co., Ltd., provided technical support for the WMT systems. Valuable comments from two anonymous reviewers helped us in improving the manuscript. This work was funded by 'The 2nd New Program of Research and Observation for Earthquake Prediction' program of the Ministry of Education, Culture, Sports, Science and Technology of Japan. All figures were prepared with the GMT provided by Wessel and Smith [1998].

References

- Caldwell, T. G., H. M. Bibby, and C. Brown (2004), The magnetotelluric phase tensor, *Geophys. J. Int.*, *158*, 457–469, doi:10.1111/j.1365-246X.2004.02281.x.
- Fuji-ta, K., T. Katsura, T. Matsuzaki, M. Ichiki, and T. Kobayashi (2007), Electrical conductivity measurement of gneiss under mid- to lower crustal P-T conditions, *Tectonophysics*, *434*, 93–101, doi:10.1016/j.tecto.2007.02.004.
- Gamble, T. D., W. M. Goubau, and J. Clarke (1979), Magnetotellurics with a remote magnetic reference, *Geophysics*, *44*, 53–67, doi:10.1190/1.1440923.
- Geological Survey of Japan (2007), Seamless digital geological map of Japan (1: 200,000), Research Information Database DB084, http://riodb02.ibase.aist.go.jp/db084/index_e.html, Natl. Inst. of Adv. Ind. Sci. and Technol., Tsukuba, Japan, 12 May.
- Glover, P. W. J., M. J. Hole, and J. Pous (2000), A modified Archie's law for two conducting phases, *Earth Planet. Sci. Lett.*, *180*, 369–383, doi:10.1016/S0012-821X(00)00168-0.
- Goto, T., Y. Wada, N. Oshiman, and N. Sumitomo (2005), Resistivity structure of a seismic gap along the Atotsugawa fault, Japan, *Phys. Earth Planet. Inter.*, *148*, 55–72, doi:10.1016/j.pepi.2004.08.007.
- Gürer, A., and M. Bayrak (2007), Relation between electrical resistivity and earthquake generation in the crust of West Anatolia, Turkey, *Tectonophysics*, *445*, 49–65, doi:10.1016/j.tecto.2007.06.009.
- Hirahara, K., Y. Ooi, M. Ando, Y. Hosoi, Y. Wada, and T. Ohkura (2003), Dense GPS array observations across the Atotsugawa fault, central Japan, *Geophys. Res. Lett.*, *30*(6), 8012, doi:10.1029/2002GL015035.
- Hyodo, M., and K. Hirahara (2003), A viscoelastic model of interseismic strain concentration in Niigata-Kobe Tectonic Zone of central Japan, *Earth Planets Space*, *55*, 667–675.
- Iio, Y., T. Sagiya, Y. Kobayashi, and I. Shiozaki (2002), Water-weakened lower crust and its role in the concentrated deformation in the Japanese Islands, *Earth Planet. Sci. Lett.*, *203*, 245–253, doi:10.1016/S0012-821X(02)00879-8.
- Ito, K., H. Wada, S. Ohmi, N. Hirano, and T. Ueno (2007), Seismic activity from routine and temporary observations of earthquakes in the northwest Chubu district, central Honshu, in *Geodynamics of Atotsugawa Fault System*, edited by M. Ando, pp.45–63, Terra Sci., Tokyo.
- Kariya, K. A., and J. Shankland (1983), Electrical conductivity of dry lower crustal rocks, *Geophysics*, *48*, 52–61, doi:10.1190/1.1441407.
- Kato, A., E. Kurashimo, N. Hirata, T. Iwasaki, and T. Idaka (2006), Imaging crustal structure around the western segment of the Atotsugawa fault system, central Japan, *Geophys. Res. Lett.*, *33*, L09307, doi:10.1029/2006GL025841.
- Mikumo, T., H. Wada, and M. Koizumi (1988), Seismotectonics of the Hida region, central Honshu, Japan, *Tectonophysics*, *147*, 95–119, doi:10.1016/0040-1951(88)90150-3.
- Nakajima, J., and A. Hasegawa (2007), Deep crustal structure along the Niigata-Kobe Tectonic Zone, Japan: Its origin and segmentation, *Earth Planets Space*, *59*, e5–e8.
- Nesbitt, B. E. (1993), Electrical resistivities of crustal fluid, *J. Geophys. Res.*, *98*, 4301–4310, doi:10.1029/92JB02576.
- Ogawa, Y., and Y. Honkura (2004), Mid-crustal electrical conductors and their correlations to seismicity and deformation at Itoigawa-Shizuoka Tectonic Line, central Japan, *Earth Planets Space*, *56*, 1285–1291.
- Ogawa, Y., and T. Uchida (1996), A two-dimensional magnetotelluric inversion assuming Gaussian static shift, *Geophys. J. Int.*, *126*, 69–76, doi:10.1111/j.1365-246X.1996.tb05267.x.
- Ogawa, Y., et al. (2001), Magnetotelluric imaging of fluids in intraplate earthquake zones, NE Japan back arc, *Geophys. Res. Lett.*, *28*, 3741–3744, doi:10.1029/2001GL013269.
- Sagiya, T., S. Miyazaki, and T. Tada (2000), Continuous GPS array and present-day crustal deformation of Japan, *Pure Appl. Geophys.*, *157*, 2303–2322.
- Siripunvaraporn, W., and G. Egbert (2000), REBOCC: An efficient data-subspace inversion for two-dimensional magnetotelluric data, *Geophysics*, *65*, 791–803, doi:10.1190/1.1444778.
- Siripunvaraporn, W., G. Egbert, and M. Uyeshima (2005), Interpretation of two-dimensional magnetotelluric profile data with three-dimensional inversion: Synthetic examples, *Geophys. J. Int.*, *160*, 804–814, doi:10.1111/j.1365-246X.2005.02527.x.
- Ueno, T., K. Ito, K. Yoshii, K. Matsumura, and H. Wada (2005), Crustal structure and seismic activity around the Atotsugawa fault system, central Honshu, Japan (in Japanese with English abstract), *J. Seismol. Soc. Jpn.*, *58*, 143–152.
- Uyeda, S., and K. Horai (1964), Terrestrial heat flow in Japan, *J. Geophys. Res.*, *69*, 2121–2141, doi:10.1029/JZ069i010p02121.
- Wannamaker, P. E. (1999), Affordable magnetotellurics: Interpretation in natural environments, in *Three-Dimensional Electromagnetics*, edited by M. Oristaglio and B. Spies, pp. 349–374, Soc. of Explor. Geophys., Tulsa, Okla.
- Wessel, P., and W. H. F. Smith (1998), New, improved version of Generic Mapping Tools released, *Eos Trans. AGU*, *79*(47), 579, doi:10.1029/98EO00426.
- Yoshimura, R., et al. (2008), Magnetotelluric observations around the focal region of the 2007 Noto Hanto Earthquake (Mj6.9), central Japan, *Earth Planets Space*, *60*, 117–122.
- K. Aizawa, S. Koyama, and M. Uyeshima, ERI, University of Tokyo, Tokyo 113-0032, Japan.
- Y. Fujita, S. Nakao, N. Oshiman, T. Uto, Y. Wada, and R. Yoshimura, DPRI, Kyoto University, Uji 611-0011, Japan.
- T. Goto, Department of Civil and Earth Resources Engineering, Kyoto University, Kyoto 615-8540, Japan.
- M. Harada, EPRC, Tokai University, Shizuoka 424-8610, Japan.
- Y. Honkura, Department of Earth and Planetary Sciences, Tokyo Institute of Technology, Tokyo 152-8550, Japan.
- H. Kanezaki, Department of Earth Sciences, University of Toyama, Toyama 930-8555, Japan.
- T. Kasaya, JAMSTEC, Kanagawa 237-0061, Japan.
- M. Mishina, RCPEVE, Tohoku University, Sendai 980-8578, Japan.
- Y. Mochido and I. Shiozaki, Department of Civil Engineering, Tottori University, Tottori 680-8550, Japan.
- T. Mogi and Y. Yamaya, ISV, Hokkaido University, Sapporo 060-0810, Japan.
- H. Murakami, Department of Applied Science, Kochi University, Kochi 780-8520, Japan.
- T. Nishitani and S. Sakanaka, Department of Earth Science and Technology, Akita University, Akita 010-8502, Japan.
- Y. Ogawa, VFRC, Tokyo Institute of Technology, Tokyo 152-8550, Japan.
- H. Satoh, Nippon Engineering Consultants Co., LTD, Tokyo 170-0003, Japan.
- H. Toh, Graduate School of Science, Kyoto University, Kyoto 606-8502, Japan.
- S. Yamaguchi, Department of Earth and Planetary Sciences, Kobe University, Kobe 657-8501, Japan.